Wetlands (2016) 36 (Suppl 2):S287–S297
DOI 10.1007/s13157-016-0817-9

ORIGINAL RESEARCH

Characterizing the Climate-Driven Collapses and Expansions of Wetland Habitats with a Fully Integrated Surface–Subsurface Hydrologic Model

Ganming Liu[1] · **Franklin W. Schwartz**[2] · **Christopher K. Wright**[3] · **Nancy E. McIntyre**[4]

Received: 3 March 2016 / Accepted: 27 August 2016 / Published online: 6 September 2016

Abstract Links between climatic forcing and wetland habitats can be conceptualized using a graph-theoretical approach, which treats wetlands as nodes to map habitat connectivity and to define habitat networks for ecological analysis. The first and most crucial step in creating a network model, however, is to characterize the dynamic behaviors of the nodes, i.e., the occurrence of wetlands with ponded water, or water bodies. For the first time, this study applies a 3-D, fully integrated surface and subsurface flow model, HydroGeoSphere (HGS), to simulate the hydrologic dynamics of wetlands in the Prairie Pothole Region (PPR) and to characterize the resulting habitat networks as a function of climate variability. Results show HGS is able to simulate water movement in both surface and subsurface domains and capture "fill-spill" and coalescence/disaggregation behaviors of wetlands as they respond to wet and dry climatic conditions. Our simulations for a small representative subarea of the PPR show wetland networks in the PPR could easily shrink, degrade, or even collapse when the climate becomes drier. This study demonstrates the potential in applying sophisticated hydrologic models to solve critical ecological problems and the practical implications for water-resources management, conservation planning and decision-making in the PPR.

Keywords Climate change · Connectivity · Drought · Habitat networks · Hydrologic modeling · Prairie Pothole Region · Wetlands

✉ Ganming Liu
gliu@bgsu.edu

[1] School of Earth, Environment and Society, Bowling Green State University, Bowling Green, OH 43403, USA

[2] School of Earth Sciences, The Ohio State University, Columbus, OH 43210, USA

[3] Natural Resources Research Institute, University of Minnesota, Duluth, MN 55811, USA

[4] Department of Biological Sciences, Texas Tech University, Lubbock, TX 79409, USA

Introduction

The 750,000 km^2 Prairie Pothole Region (PPR) of the northern Great Plains is the breeding area for more than half of North American migratory waterfowl due to the occurrence of millions of closed-basin pothole lakes and wetlands scattered across the landscape (Sloan 1972; Larson 1995). Formed by glacial processes, these water bodies rely on rainfall and snowmelt for water and are highly variable in surface area, depth, and hydroperiod. These water bodies are considered one of the most ecologically valuable freshwater resources of the United States (U.S.) (Guntenspergen et al. 2006) and are sensitive to temporal fluctuations in climate. For example, our recent studies (Zhang et al. 2009; Liu and Schwartz 2011, 2012) have shown that numbers of water bodies in South and North Dakota might fluctuate more than one order-of-magnitude in response to the inter-annual cycling between drought and deluge. Such variability in the hydrologic response of potholes naturally impacts productivity of waterfowl dependent on these habitats and points to the extreme risk associated with projected climate change.

There has been a recent emphasis on new strategies for describing and evaluating the quality of wetland habitats for wildlife. One of the most compelling approaches involves the application of graph theory (Minor and Urban 2007) to establish links between climatic drivers and habitat connectivity (e.g., Wright, 2010; McIntyre et al. 2014). Habitat

connectivity is a landscape attribute critical to preserving biodiversity in the face of climate change. It describes the ability of species to disperse or move between patches of suitable habitat. For wetland-dependent species, movements between wetlands involve a range of spatial scales, and involve activities such as foraging within wetland complexes, dispersal of young-of-the-year from natal sites, bird migration along the Central Flyway, dispersal to newly available habitat during deluge and migration to drought refugia during dry times. Such movements are critical to long-term persistence (Haig et al. 2008) and will influence species range adjustments to climatic shifts. Compared to continuously varying habitat types, e.g. gradations of forest or grassland, PPR wetlands and lakes represent spatially discrete habitat patches. Thus, PPR landscapes are ideally suited to a graph-theoretical treatment, with wetlands/lakes forming the nodes of a graph and linkages, or edges, representing potential pathways for movements among them (Fig. 1). Such a graphical approach can rapidly quantify habitat availability, which is crucial in monitoring changes in naturally dynamic landscapes like the PPR, and is even more important given the unprecedented dynamics being imposed on water resources by climate change.

To apply the graph-theoretic approach to define wetland networks and to determine potential habitat connectivity across landscapes, the first and most essential step is to identify nodes on the landscapes, which requires spatially explicit information, e.g., X (longitude or UTM easting) and Y (latitude or UTM northing) values for wetland centroids. Satellite imagery has proven to be invaluable for this purpose by providing large-scale data-sets for monitoring the hydrologic character of wetlands and lakes and patterns of change in the PPR (e.g., Zhang et al. 2009; Wright, 2010). However, using these kinds of data come with certain limitations, for examples, the relatively short duration of observational records, their modest spatial resolutions, and the inability to provide direct quantitative information with respect to water transfers (Liu and Schwartz 2011).

Models can be used to leverage such satellite-based observations. Models provide a way to explore the behavior of hydrologic systems in terms of underlying processes and parameters and to extrapolate system behaviors backwards or forwards in time to evaluate historic and future stresses. As is well known, climate varies widely over time scales of decades to centuries (e.g., Woodhouse and Overpeck 1998; Laird et al. 2003) but the imagery available for analysis only represents the more modern history of wetland response to climate fluctuations. Studies have shown that approaches integrating satellite-based observations of lake/wetland systems together with hydrologic models have been particularly useful in studying the longer-term behavior of water bodies in the PPR. For example, Liu and Schwartz (2011) developed a pothole complex hydrologic model (PCHM) that is capable of simulating the hydrologic behavior of lake-wetland complexes that included tens of thousands of water bodies. The model was applied to elucidate the behaviors of a large complex of potholes along the Missouri Coteau in North Dakota and to describe how water-body numbers and areas fluctuated in response to climate variability through the twentieth century. This time period captured decadal impacts of drought in the 1930s and the deluge of the late 1990s. Models, moreover, have the ability to predict how wetlands will respond to future climatic scenarios. For instance, Wright et al. (2016) used a spatially-explicit version of PCHM to simulate wetland network dynamics under projected climate change.

Another hydrologic model that has been used successfully in modeling pothole-type wetlands is WETSIM and its successor, WETLANDSCAPE (or WLS; Poiani et al. 1996; Johnson et al. 2010; Johnson and Poiani 2016). This model provides the capability to simulate the dynamic response of wetland complexes in terms of surface water, groundwater, and successional vegetation dynamics. Yet, PCHM, WETSIM, and WLS are all somewhat limited by simplifications that come along with bucket-type hydrologic models. There are difficulties in handling spatial features of the

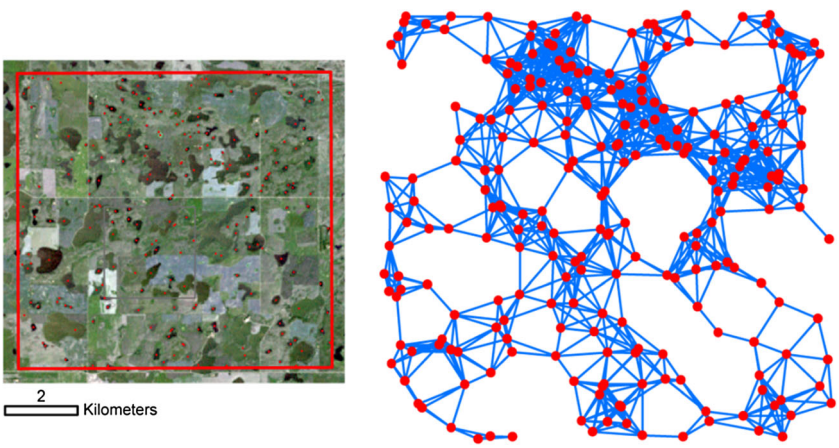

Fig. 1 A wetland landscape in central North Dakota (*left*) and the associated network (*right*) created with a graph-theoretical approach. Circles represent nodes (i.e., centroids of wetlands) and lines represent links between nodes that have a distance less than a threshold value or disperse distance of 1000 m

wetland networks and hydrologic processes, such as the coalescence of neighboring wetlands during wet periods, disaggregation during dry periods, and/or influence of surface-water and groundwater movement among water bodies in larger scale groundwater flow settings. In addition, it has been a challenge to model "fill-spill" dynamics that can be important in driving surface-water connectivity in prairie wetlands (Shaw et al. 2012). Because the graph-theory approach requires spatially explicit information on the occurrence of wetlands to map habitat connectivity (Fig. 1), lumped or even semi-lumped models have obvious limitations in simulating these types of behaviors, so important for this study. The use of a fully distributed hydrologic model would be a natural and ideal improvement in process representation.

Thus, the novelties in this paper include demonstrations of: (1) the potential of a 3-D fully integrated surface and subsurface flow model, HydroGeoSphere or HGS (Therrien et al. 2010; Aquanty 2015) to simulate the hydrologic dynamics of pothole lakes and wetlands; and (2) the integration of HGS modeling results into a graph theory approach to demonstrate potential drought effects on wetland habitat connectivity. Unlike the lumped models just described which are founded on empirical equations, HGS is capable of simulating the flow of water, above and below the ground surface in a physically-based manner that relies on coupled differential equations. The output from HGS provides a spatial-temporal characterization of the occurrence of water in the terrestrial hydrologic cycle, measured in terms of hydraulic head in groundwater, soil moisture, stream discharge, water depths in lakes and wetlands, evaporation/evapotranspiration, etc. In particular, the hydrologic behavior of lakes and wetlands is determined explicitly by topographic setting (i.e., digital elevation model or DEM) and climate. In other words, lakes and wetlands form in irregularly shaped depressions when hydrologic conditions favoring the accumulation of water exist. This approach lets explicit features of the topographic setting and land use/land cover also come into play in characterizing the dynamics of nodes in wetland networks.

Our first objective was to describe and demonstrate the application and efficacy of HGS in elucidating climate-driven behaviors of pothole wetlands and their connections to groundwater systems. Our second objective was to demonstrate how HGS outputs would facilitate assessment of climatic forcing on wetland habitat connectivity of areas representative of the PPR. Our particular interest in this respect was to examine how wetland habitat networks collapse and expand as a function of a highly variable climate in the PPR. We expect that results and findings presented here will contribute to a better understanding of links among climatic drivers, habitat connectivity, and management of water resources and wildlife in the PPR.

Methods

Integrated Surface and Subsurface Flow Modeling

Distributed hydrologic models have created new capabilities for simulating hydrologic systems in a way that accommodates complexity arising from processes, parameters, and system architecture (e.g., Yu and Schwartz 1998; Kollet and Maxwell 2006; Yu et al. 2006). Of the available models, HGS has been successfully used in studies around the world (e.g., Partington et al. 2013; Frei and Fleckenstein 2014; Ala-aho et al. 2015; Hwang et al. 2015). HGS works by taking rainfall and snowmelt, and effectively moving the resulting water through the land-based hydrologic cycle considering (i) processes like overland and surface-water flow, gravity-driven groundwater flow, evaporation/evapotranspiration, and infiltration, and (ii) storage in lakes, wetlands and groundwater (Aquanty 2015). HGS can accommodate variability in key parameters like precipitation, hydraulic conductivity, topography, vegetation, etc.

Surface flow in HGS is simulated using the 2-D depth-averaged diffusion-wave approximation provided by the Saint Venant equation. For saturated/unsaturated subsurface flow, HGS solves Richards equation in three dimensions. The transfer of water from one domain to another, for example, coupling surface and subsurface flows, is represented by Darcy flux (Aquanty 2015). HGS differs from other comparable models, such as GSFLOW (Markstrom et al. 2008), in not requiring pre-defined nodes for rivers or streams, which assumes that the extents of the surface waters would fluctuate within the node system. HGS provides for the natural ponding of water when the hydraulic heads are higher than the elevation of the land surface and other inflow sources to depressions are sufficient to produce standing water (Aquanty 2015; Ala-aho et al. 2015). Readers interested in a more detailed description of the model formulation, numerical implementations and other features should refer to the HGS manual (Aquanty 2015).

Study Sites and Model Setup

In this study, HGS was applied to simulate the cycling of water within two wetland landscapes. The first was a synthesized wetland landscape (SWL) with depressions of varying sizes representing the heterogeneous wetlands of the PPR. A hummocky topography (Fig. 2) that is representative of conditions in parts of the PPR was generated using a reciprocal distance covariance model (Huang 2012). The model domain was square, 1000 m × 1000 m, with land-surface elevations that range from 20.0 m to 33.8 m (Fig. 2). A plane with a constant elevation of 0 m formed the bottom of the domain. The domain was discretized areally by a regular, square grid with a uniform spacing (ΔX, ΔY = 10 m) and vertically with

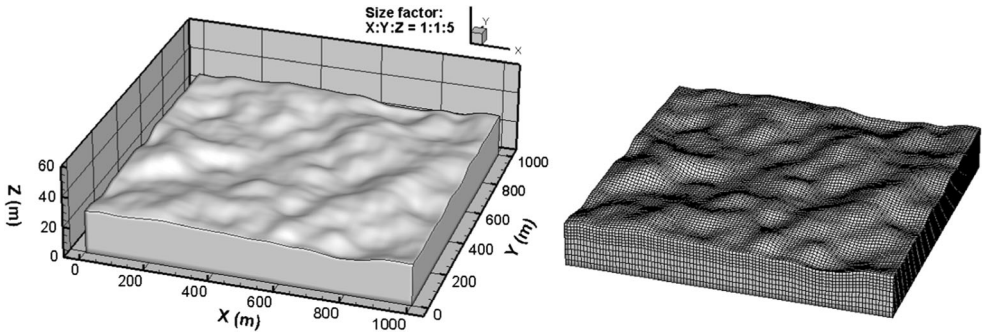

Fig. 2 Synthesized wetland landscape (*left*) and its discretization (or domain mesh, *right*) for HydroGeoSphere simulation

10 layers. The upper five layers had a thickness of 2 m and the lower five layers evenly divided the remaining thickness. In total, there were 100,000 elements and 112,211 nodes.

The modeling of the synthesized landscape was designed to examine the extent to which HGS was able to capture the dynamics of the wetland behavior in response to climate variations. Of particular interest was simulating the behavior of ponded water in wetlands as climate became wetter and/or drier. For simplicity, we assumed no-flow boundaries on all four sides and the bottom of the domain. The top boundary provides for fluxes of water to enter or leave the domain either as specific recharge, i.e., rainfall or evapotranspiration (ET), when drying is indicated. The initial condition for the surface and subsurface systems assumed a water Table 2.0 m below the land surface, and the initial water depth of surface waters set to a value close to zero (1.0×10^{-4} m), indicating a dry condition. The aquifer was assumed to be homogenous, with a horizontal saturated hydraulic conductivity (or K_h) of 2.0×10^{-4} cm/s or 0.173 m/d and vertical hydraulic conductivity (or K_v) of 2.0×10^{-5} cm/s.

A second application of HGS involves the simulation of an actual or realistic wetland landscape (RWL) in the PPR of central North Dakota, at the site of the U.S. Geological Survey Cottonwood Lake Study Area (Fig. 3). Detailed descriptions of the geology, hydrology and climatology of this study area are provided by Winter (2003) and our previous studies such as Liu and Schwartz (2011) and Gong et al. (2015). The RWL simulation domain had a dimension of 2500 m × 2500 m, which was discretized by a uniform, 100 × 100 square grid. Land-surface DEM data (1/3 arc-second or approximately 10-m resolution) came from the National Elevation Dataset, available at http://viewer.nationalmap.gov/viewer/. As shown in Fig. 3, the land surface across the RWL was hummocky with elevations varying from a high of 588.7 m above sea level (m.a.s.l.) to a low of 546.3 m.a.s.l. (Fig. 3). The base of the domain was set at an elevation of 530 m.a.s.l. with the domain discretized vertically into six layers. Layer thicknesses increase from the ground surface downward. The uppermost two layers were 1.5 m thick; the third and fourth layers were 2 m and 4 m thick, respectively; and the lowermost two layers extended to the bottom of the domain with a ratio in thickness of 1:1.5 (Fig. 3). In total, the model grid contained 60,000 elements and 71,407 nodes.

The focus with the second model was to explore how a landscape and wetland complex in nature responds to extreme climatic conditions or events. Compared to the first example of modeling with the synthesized landscape which aimed to test HGS's capability in handling key hydrologic processes in the 3D domain (e.g., surface and subsurface flows and surface-subsurface interactions), this second case is more realistic. For example, it incorporates more hydrologic complexities, such as the heterogeneity of the subsurface, actual topography for overland flow, and snowmelt. Nevertheless, we have not attempted to build a faithful replica of the system at Cottonwood Lake Study Area. This level of complexity is beyond the scope of the present paper.

The boundary conditions were similar to the previous case and the initial condition for this second demonstration was achieved by spinning up the model with a normal climatic condition. In both cases, the HGS model was driven by climate variables such as rainfall, ET, temperature, and snowmelt (RWL case only) and took advantage of adaptive time stepping to reduce execution time. An initial time step of 0.1 day was used. Depending on the modeling purposes, the climate data used varied and are described in their respective sections. Values of some key HGS model parameters and settings are summarized in Table 1. Default values for other necessary parameters were adapted from the HGS manual (Aquanty 2015). Note that model parameters were not calibrated in this study. For convenience, abbreviations SWL and RWL were used to represent the model settings of the synthesized and realistic landscape cases, respectively.

Results

Groundwater/Surface-Water Interaction in Wetland Systems

The SWL based simulation was performed to examine HGS's capability in modeling the 3-D surface and subsurface flows and interactions. Specifically, we examined how surface water

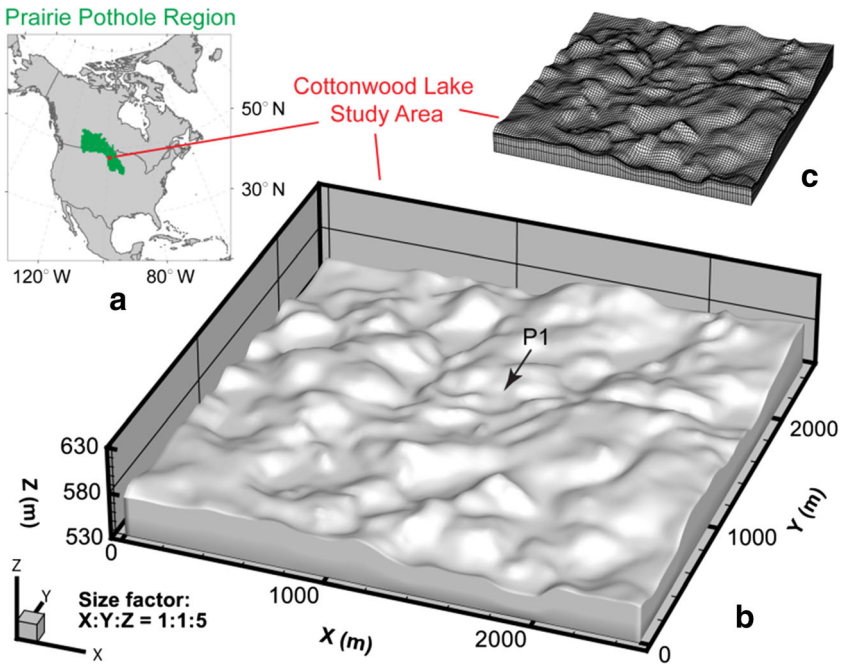

Fig. 3 Location **a**, topography **b**, and domain discretization **c** of the wetland landscape covering the U.S. Geological Survey Cottonwood Lake Study Area. The *green* area in panel **a** is the Prairie Pothole Region of North America

occurs or ponds on the land surface simply due to the interaction between groundwater and surface water. In this case, therefore, zero recharge (no rainfall or snowmelt), ET, or runoff was applied to the land surface. Note that the initial surface-water depth was close to zero, meaning that there was no ponded water in the depressions. The initial water table was set to 2 m below ground surface, thus creating hydraulic gradients capable of moving groundwater water from the topographic highs to depressions, thereby forming lakes and wetlands.

Figure 4 shows the occurrence of surface water (displayed as water depth). Note how surface-water bodies began to form and grew through time as groundwater flowed into the depressions. At the beginning of the simulation (Day 0), there was no surface water (Fig. 4a). After 100 days, several surface-water bodies became evident due to inflows from groundwater (Fig. 4b). As time continued, these water bodies expanded, while other new water bodies formed (Fig. 4c-e).

Notable features of this HGS simulation are the tendency for nearby water bodies to coalescence and for fill-and-spill

Table 1 Values of select HydroGeoSphere model parameters. SWL = synthesized wetland landscape. RWL = realistic wetland landscape

	Parameter (unit)	Values (SWL)	Values (RWL)
Porous medium	Saturated hydraulic conductivity		
	K_h (m/d)	0.173	[a]0.173; 0.173; 0.0173; 0.0173; 0.0173; 0.0173
	K_v (m/d)	K_h/10.0	K_h/10.0
	Specific storage (1/m)	1.0×10^{-4}	1.0×10^{-4}
	Porosity	0.25	0.25
	Van Genuchten α	3.0	3.0
	Van Genuchten β	2.5	2.5
	Residual water saturation	0.0633	0.0633
Overland flow	Manning's n in x and y ($s/m^{1/3}$)	0.2	0.2
	Rill storage height (m)	0.02	0.02
	Obstruction storage height (m)	0.02	0.02
	Coupling length (m)	0.01	0.01
Evapotranspiration	Evaporation depth (m)	0.2	0.2
	Root depth (m)	1.5	1.5
	Lead area index, or LAI	1.0	1.0

[a] The six numbers represent the K values of six vertical layers from top to bottom

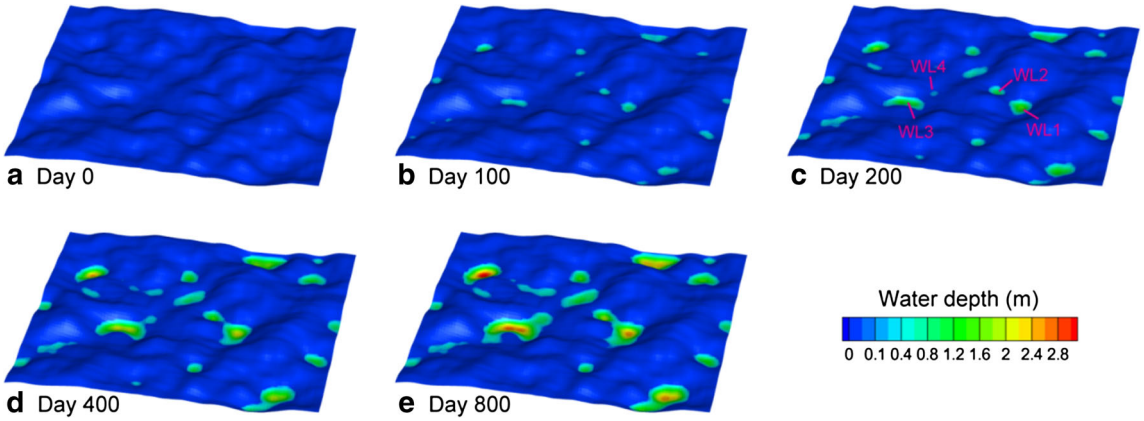

Fig. 4 Occurrence of surface-water bodies on the synthesized wetland landscape (1000 m × 1000 m) simulated by using HydroGeoSphere. Four wetlands (WL1, WL2, WL3, and WL4) are denoted

processes to accelerate this process. For example, WL1 and WL2 were two individual wetlands on Day 200 (Fig. 4c). By Day 400, the two water bodies have coalesced (Fig. 4d). A detailed examination of the filling process indicates that groundwater feeding both of the wetlands first filled the wetland situated at a higher elevation, i.e., WL2. Once spilling began, the groundwater discharge to WL2 was added to topographically lower WL1, increasing the groundwater already flowing into that water body. Once the stage was the same, the two water-bodies have coalesced into one. WL3 and WL4 shown on the figure behave in the same way.

Because this example did not include a precipitation component, the formation and expansion of surface-water bodies (Fig. 4) were simply caused by their interactions with groundwater through flux exchange. Figure 5 displays the spatial and temporal patterns in fluxes, as estimated by HGS. The magnitude of the fluxes depended on hydraulic conductivity and hydraulic gradient existing between the water bodies and adjacent groundwater. A positive exchange flux indicates that water was flowing into depressions from the groundwater. A negative exchange flux indicates just the opposite. At an early time (Day 50, Fig. 5a), the exchange fluxes were large in magnitude (greater than 0.0045 m/d) and positive, pointing to relatively large inflows of groundwater to the major depressions. Not surprisingly, the largest gradients were associated with the deepest depressions. With time, fluxes became smaller as the increasing stage of the surface-water bodies and declining water-table elevations effectively reduced the hydraulic gradients. However, the areas over which flux was occurring increased in time due to the increasing area of the wetland surface.

Exchange fluxes were highest near wetland perimeters, particularly on those sides associated with highlands (e.g., WL1 and WL3; Fig. 5b). Near the shore, fluxes were higher because at those locations gradients were maximized. Because stage was constant, moving a greater distance from shore effectively reduced the hydraulic gradient. As the simulation extended to day 400, some negative flux values began to show up. Groundwater was not being recharged, so locally water tables might become lower than the stage of some nearby water body. This behavior was evident with WL5 (Fig. 5c), where the flux was negative on the side of the water body

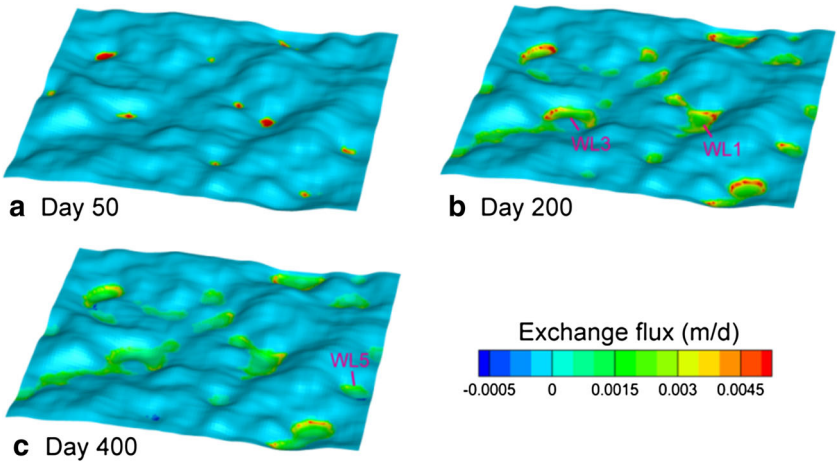

Fig. 5 Spatiotemporal patterns of groundwater and surface-water interactions. A positive value of the subsurface/surface exchange flux indicates groundwater inflow to water bodies, whereas a negative value indicates outflow to the groundwater. Three wetlands (WL1, WL3, and WL5) are denoted

away from the local highland. WL5 then was an example of a flow-through lake as described by Winter (1978).

Response of Wetland Landscape to Variability in Climatic Conditions

To explore how a wetland landscape responds to hypothetical variability in climatic conditions, fluxes of water across the top boundary, representing the influence of rainfall and evapotranspiration, were varied through a SWL simulation. Specifically, during a 1000-day simulation, fluxes were adjusted to provide a pulse in rainfall, increasing from 0.0 to 0.002 m/d at Day 200 and returning back to 0.0 m/d at Day 400 (Fig. 6a). Potential evapotranspiration (PET) was assumed to be a step function increasing from 0.0 to 0.004 m/d at Day 400 and continuing to Day 1000 (Fig. 6a). As with the previous model run, at time zero, there was no surface water initially present, but groundwater was available to discharge to the surface once the simulation started.

The continuous precipitation from Days 200 to 400 added extra water to the domain (compared to the previous case with zero precipitation over Days 200–400), increased the groundwater recharge, and generated overland flow when there was excess water, causing the land surface to become particularly wet (Fig. 6b-d). A cross-comparison to the pattern for Day 400 in the zero-recharge case (Fig. 4d) shows more water bodies with a greater depth and area (Fig. 6d). At the end of this wetting period, i.e., Day 400, WL3 had become a large water body with a maximum water depth > 3.5 m.

At Day 400, the precipitation was halted and evaporation was turned on, to provide a drying period with persistent negative effective moisture, i.e., rainfall minus PET <0. Driven by the drier weather, water bodies started to lose much of their water via evaporation/evapotranspiration, and both the number of water bodies and their size declined greatly (Fig. 6e and f). By the end of the simulation on Day 1000, there were just a few surface-water bodies remaining in lowlands (Fig. 6f).

The shift in climatic conditions also drove changes in the character of surface-subsurface interaction. With wetter conditions, the fluxes at the ground surface were positive (right panels, Fig. 6c and d), indicating that lakes and wetlands gained water from the groundwater system. With drier conditions, the surface fluxes in contrast turned negative (right panels, Fig. 6e and f), indicating that wetlands not only lost water to the atmosphere via evaporation, but to the subsurface via leakage.

Creating Wetland Networks with Simulated Surface-Water Occurrence

The next HGS simulation moved from the synthesized wetland topography (Figs. 4, 5 and 6) to a more realistic representation of an actual landscape (Fig. 3). It afforded the opportunity to

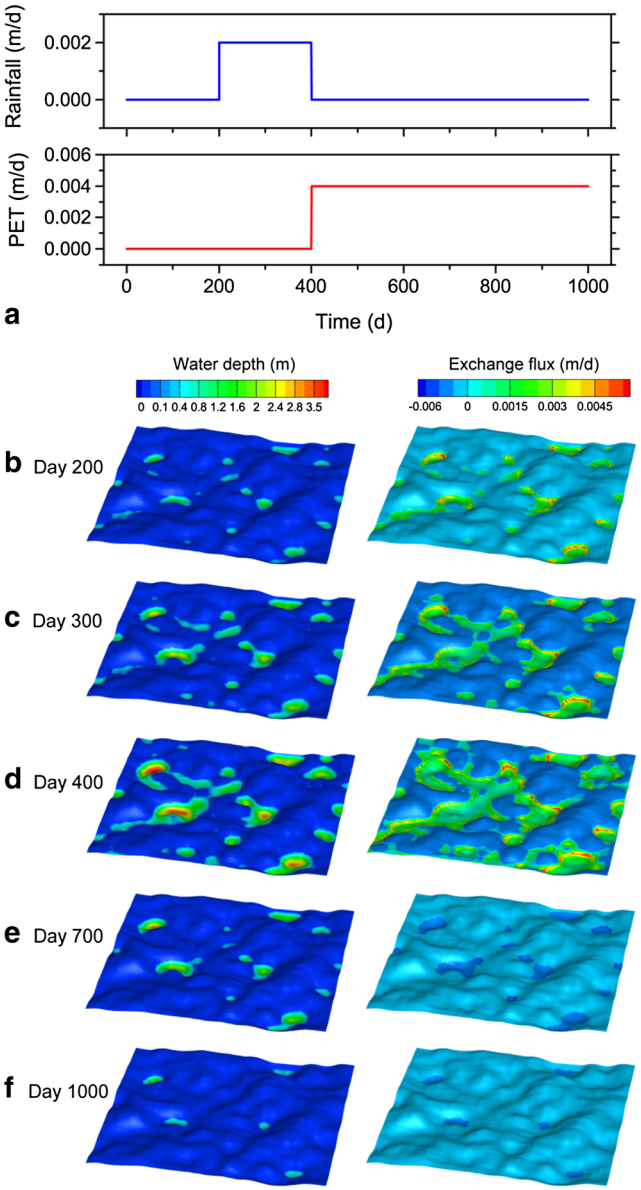

Fig. 6 Responses of surface waters on a synthesized wetland landscape to variability in weather through time. Panel **a** displays the time series of rainfall and potential evapotranspiration (PET) and panels **b**-**f** show the spatiotemporal patterns of surface-water depth (*left*) and exchange fluxes between surface and subsurface (*right*)

investigate landscape connectivity as a function of climatic variability over a ten-year period, i.e., 1991–2000. Monthly climate data, including rainfall, snow, temperature and PET, were processed and inputted as daily records to drive the HGS model. Rainfall, snow and temperature data were obtained from the Global Historical Climatology Network (available at http://www1.ncdc.noaa.gov/pub/data/ghcn). PET was calculated using the FAO Penman-Monteith method (Allen et al. 1998; Liu and Schwartz 2011). As indicated, the model was spun up to begin in 1991 with proper initial conditions.

Good comparability in the sizes of observed (from Landsat satellite images, Fig. 7a) and simulated (Fig. 7b) surface-water

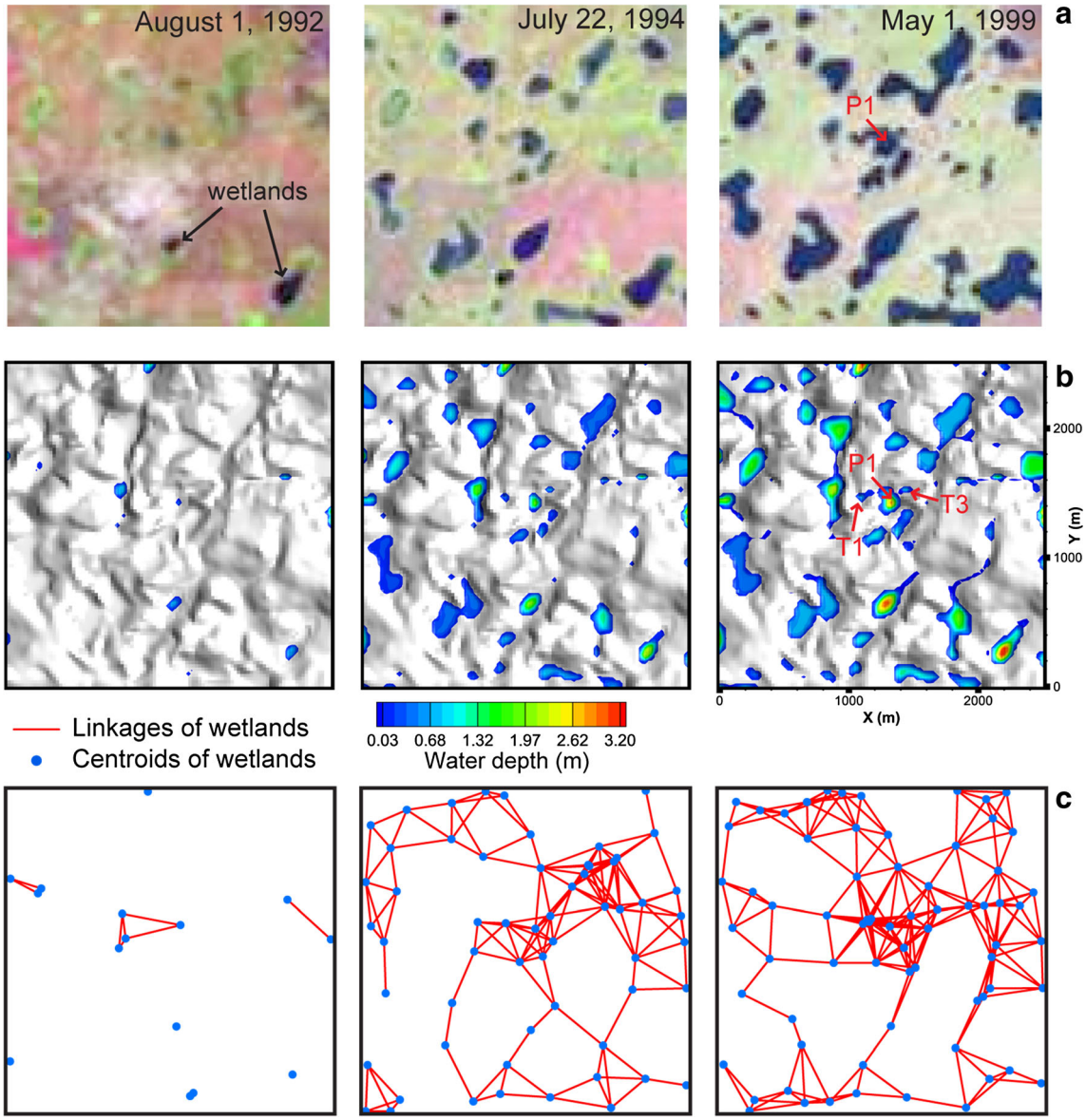

Fig. 7 Wetland habitat networks assembled using the simulated distribution of water bodies within a 2.5 × 2.5 km area in central North Dakota. Panel **a** shows Landsat satellite images of the area from August 1992 (dry climatic condition), July 1994 (wet), and May 1999 (wetter). Panel **b** shows the simulated surface water (as depth) for the same months. The resulting wetland networks are shown in Panel **c**. *Blue* nodes are centroids of water bodies. *Red lines* are linkages or possible directions of movements between the water bodies. The networks were created by using a dispersal distance of 500 m. Three wetlands (P1, T1, and T3) are denoted

bodies suggested that the hydrologic model captured climate-driven dynamics of the wetlands. In August 1992, the landscape was dry and with very few water bodies (left, Fig. 7a and b), due to a drought that began in 1988. By July 1994, the landscape had recovered from the drought and contained many more water bodies (middle, Figs. 7a and b). The wetter condition was brought about by an extremely moist summer in 1993 during which there was unusually high precipitation (over 27 cm) in July. In May 1999, more water bodies are visible from both the satellite image (right, Fig. 7a) and from the simulated water-depth plot (right, Fig. 7b) as a result of the influence of continuously wet conditions.

A realistic simulation of the surface-water occurrence in space and time (Fig. 7b) provides the necessary information to apply graph theory in the analysis of the network. Such a network essentially describes the potential ecological connectivity among the discrete wetlands for the three different climatic conditions represented during the 10-year simulation (Fig. 7c). In this case, centroids of wetlands were located and linked by using a dispersal distance of 500 m. In other words, wetlands located within 500 m of each other were connected. This distance was chosen as it represents localized movements, e.g., for amphibians (e.g., frogs and toads, Mushet et al. 2012) or daily foraging movements of larger

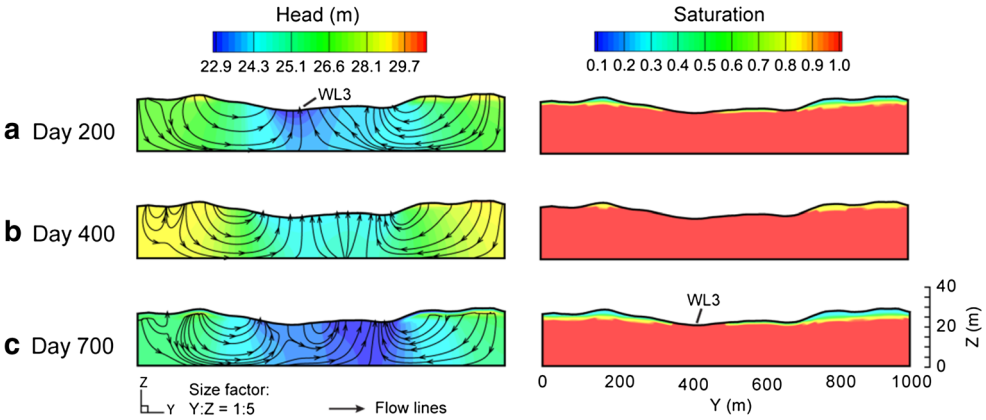

Fig. 8 Cross-sectional profiles (extracted at X = 350 m) showing the distribution of hydrologic heads (*left*) and saturation (*right*) for the case represented in Fig. 6. The flow lines were generated based on the heads shown in the cross sections and may not be exactly as the flow lines in the 3-D domain

wetland-associated animals. Using a larger dispersal distance would result in more wetlands being aggregated into clusters of potentially accessible habitat.

Figure 7c shows that in 1992, the drought conditions clearly affected ecological connectivity. The network itself was comprised of a few isolated nodes and barely connected. At a dispersal distance of 500 m, the ecological connectivity had collapsed (left, Fig. 7c). With the drought broken by heavy rains in summer of 1993, the water bodies quickly increased in size and number. The result by 1994 was a much more robust network with most water bodies well connected, except a few in the lower-left corner. With a general continuation of wet conditions through 1999, an increasing number of water bodies were interconnected by a single, expanded network. Indeed, ecological connectivity analyses based on the three resulting networks indicated a 386 % increase in the number of surface-water bodies from 1992 to 1999. The result was a concomitant increase in the number of linkages among water bodies during the wettest period, and a decrease in the distance that an animal would need to travel, going from wetland to wetland, to traverse the landscape (i.e., the coalescence distance). An animal moving through the wettest landscape would need to travel only a third as far as one in the driest landscape to find a waterbody. Our results shown in Fig. 7c clearly indicate the significant impact that climate-driven variability can produce in terms of wetland habitat connectivity.

Discussion and Conclusions

The HGS model provides an alternative approach for simulating the occurrence of water bodies as a function of climate. As the results in Fig. 7 demonstrate, this information can form the basis for an examination of the hydrologic function of prairie pothole lake/wetland complexes. With HGS, we have been able to capture some of the complex behaviors of wetlands and lakes as the outcome of key hydrologic processes. Examples include time varying rainfall and evapotranspiration, overland and groundwater flows, surface water and groundwater interactions, and limnological complexities related to inter-connection of surface-water bodies. For example, "fill-spill" behaviors can lead to rapid changes in water level adjustments to the surface-water connectivity in the prairie wetland region (Shaw et al. 2012). The fine-grained, hummocky character of the topography in some parts of the PPR has made describing the fill-spill processes especially challenging in relation to prairie lake and wetland complexes. HGS is able to simulate such complexity by virtue of its distributed, physically-rigorous approach in modeling the water cycle. The lumped model approaches developed in our previous studies (e.g., Liu and Schwartz 2011) could not represent the coalescence and disaggregation behaviors associated with surface-water complexes.

Results from this study imply that contributions from surface water and groundwater are essential for lakes and wetlands to maintain standing water in their basins, especially during drier summer months and inter-annual drought conditions. Lakes and wetlands in lowlands have the potential to gain some amounts of water via groundwater discharge, and commonly demonstrate resistance to drought. Water gained from groundwater inflows during dry periods can offset strong evaporative losses to some extent (Fig. 4). Thus, water-body storage can be maintained for some time even with significant evaporation (Figs. 6e-f).

The fully integrated treatment of surface and subsurface water in HGS facilitates the accurate quantification of the interaction and flux exchange between those domains. One finding of particular interest is that the mode of interaction between surface waters and groundwaters could switch as a response to changes in climatic conditions. For example, positive exchange fluxes (lakes/wetlands gaining water from subsurface) tended to occur with wet conditions; whereas negative exchange fluxes were found when conditions became drier (right panels, Fig. 6).

To illustrate the possibilities for the flux reversals between groundwater and surface water, we have plotted results from HGS (SWL) as a vertical cross-section. Figure 8 shows the hydraulic head distribution, patterns of groundwater flow, and

water saturation along a north-south cross-section at X = 350 m and passing through WL3. In the wetting process (Fig. 8a-b), both water table (top boundary of the red-colored saturation zone) and surface-water level (e.g., head value at WL3) rose and groundwater flows discharged at WL3. In other words, WL3 was a "gaining" wetland that received groundwater discharge. When climate became very dry (Fig. 8c), the water table to the right of WL3 fell to a level that was lower than the stage for WL3. This lowering caused some groundwater to flow laterally, away from WL3 towards the right (Fig. 8c). In this setting then, WL3 became a "flow-through" water body which gained water from aquifer on the left side and lost water to the right.

To the best of our knowledge, this study represents the first example where the results of 3-D hydrologic modeling have been linked with graph theory to ascertain the effects of drought and deluge on ecological connectivity. Our network analysis based on the HGS results illustrated broad differences in network connectivity, ranging from near total fragmentation of wetlands to strong ecological connectivity, as the climate varied from drought to deluge. These preliminary results clearly suggest that wetland habitats in the PPR are sensitive to climate variability and that in the future drying beyond historical norms could be a critical threat to wetland habitat connectivity. An obvious next step in research is the use of climate models to assess how the networks might change over the rest of the century. Such results provide new information and understanding of the ecohydrology of complex wetland systems and have important implications for regional scale conservation planning and decision-making in the PPR.

The use of distributed water-cycle models in assessing wetland habitat connectivity presents a new direction in the application of such models. In conducting our studies, however, some limitations or challenges are worth noting. HGS does not have a graphical user interface (GUI) and has a relatively steep learning curve. Due to the complex array of coupled processes that models like HGS incorporate, model execution time and calibration are problematic. For example, our simulations were performed with a paralleled version of HGS, running on a quad-core desktop PC (3.4 GHz CPU, 16 GB RAM). A single 10-year simulation of the RWL case took nearly 20 days to execute. This long simulation time could be related to the large number of nodes (71,407 in total), the complexity of surface/subsurface hydrologic processes being simulated (Frei and Fleckenstein 2014), and/or poor optimization of parameters controlling the matrix solver in the code. The more serious limitation comes with the inability to properly calibrate the model, which of necessity requires multiple (tens, hundreds to even thousands) model runs. Thus, rigorous calibration of our realistic case study was not possible.

A second challenge related to execution times comes with the need to define an appropriate set of initial conditions for a simulation. The usual approach is to "spin-up" the model, essentially providing the model state variables through simulation. Recent studies suggest that a hydrologic system in a low permeability, arid setting could require spin-up times that are long, perhaps decades or more (e.g., Ajami et al. 2014; Gong et al. 2015). Besides the uncertainty in not knowing the length of spin-up required, there is the computational burden associated with the spin-up time. In this study, several weeks were required to find an initial condition for the RWL case. Note as well that each change in model parameter during a calibration requires yet a new spin-up.

Not surprisingly, a rigorous, spatially distributed model carries with it an enormous burden in required data. In most cases, unsaturated zone parameters are non-existent in study areas. The situation is often better for the groundwater parameters, but commonly there are insufficient data to characterize spatial variability. Lakes in particular pose special problems because there is no good way to remotely establish bathymetry and hydraulic parameters in bottom sediments. In our simulations, for example, we found that errors in water-depth estimation obviously affected ecological connectivity. For example, the coalescence of wetland P1 with two neighboring wetlands (T1 and T3) in 1999 (Fig. 7a) was not captured by our simulated water-depth results (Fig. 7b).

In summary, integrated fully 3-D modeling with HGS has contributed to characterizing and understanding the dynamics of wetland habitat connectivity in the PPR. The model is able to capture complex surface and subsurface hydrologic processes, as well as surface-water and groundwater interactions.

Acknowledgments This study was supported by the National Science Foundation awards 1340648, 1544083, and 1340548 (MacroSystems Biology Program). The authors thank Drs. Young-Jin Park, Jianming Chen, and Steven Berg for their valuable assistance with the HydroGeoSphere model. Thanks also to two anonymous reviewers and Dr. David Mushet of U.S. Geological Survey for their constructive and valuable comments on this manuscript.

References

Ajami H, McCabe MF, Evans JP, Stisen S (2014) Assessing the impact of model spin-up on surface water-groundwater interactions using an integrated hydrologic model. Water Resources Research 50:2636–2656

Ala-aho P, Rossi PM, Isokangas E, Klove B (2015) Fully integrated surface-subsurface flow modelling of groundwater-lake interaction in an esker aquifer: model verification with stable isotopes and airborne thermal imaging. Journal of Hydrology 522:391–406

Allen RG, Pereira LS, Raes D, Smith M (1998) Crop evapotranspiration: guidelines for computing crop water requirements, FAO irrigation drainage paper 56. Food Agriculture Organization, Rome

Aquanty (2015) HydroGeoSphere user manual (release 1.0). Aquanty Inc., Waterloo

Frei S, Fleckenstein JH (2014) Representing effects of micro-topography on runoff generation and sub-surface flow patterns by using superficial rill/depression storage height variations. Environmental Modelling and Software 52:5–18

Gong Y, Liu G, Schwartz FW (2015) Quantifying the response time of a Lake–groundwater interacting system to climatic perturbation. Water 7:6598–6615

Guntenspergen GR, Johnson WC, Naugle DE (2006) Prairie wetlands and climate change - droughts and ducks on the prairies. US Geological Survey Fact Sheet 2006–3144. Available at http://www.pwrc.usgs.gov

Haig SM, Mehlman DW, Oring LW (2008) Avian movements and wetland connectivity in landscape conservation. Conservation Biology 12:749–758

Huang O (2012) Terrain corrections for gravity gradiometry. Ph.D. Dissertation, The Ohio State University, Columbus. Retrieved from https://etd.ohiolink.edu/

Hwang HT, Park YJ, Frey SK, Berg SJ, Sudicky EA (2015) A simple iterative method for estimating evapotranspiration with integrated surface/subsurface flow models. Journal of Hydrology 531:949–959

Johnson WC, Poiani KA (2016) Climate change effects on prairie pothole wetlands: findings from a twenty-five year numerical modeling project. Wetlands. doi:10.1007/s13157-016-0790-3

Johnson WC, Werner B, Guntenspergen GR, Voldseth RA, Millett B, Naugle DE, Tulbure M, Carroll RWH, Tracy J, Olawsky C (2010) Prairie wetland complexes as landscape functional units in a changing climate. Bioscience 60:128–140

Kollet SJ, Maxwell RM (2006) Integrated surface-groundwater flow modeling: a free-surface overland flow boundary condition in a parallel groundwater flow model. Advances in Water Resources 29:945–958

Laird KR, Cumming BF, Wunsam S, Rusak JA, Oglesby RJ, Fritz SC, Leavitt PR (2003) Lake sediments record large-scale shifts in moisture regimes across the northern prairies of North America during the past two millennia. Proceedings of the National Academy of Sciences 100:2483–2488

Larson DL (1995) Effects of climate on numbers of northern prairie wetlands. Climatic Change 30:169–180

Liu G, Schwartz FW (2011) An integrated observational and model-based analysis of the hydrologic response of prairie pothole systems to variability in climate. Water Resources Research 47:W02504. doi:10.1029/2010WR009084

Liu G, Schwartz FW (2012) Climate-driven variability in lake and wetland distribution across the prairie pothole region: from modern observations to long-term reconstructions with space-for-time substitution. Water Resources Research 48:W08526. doi:10.1029/2011WR011539

Markstrom SL, Niswonger RG, Regan RS, Prudic DE, Barlow PM (2008) GSFLOW-coupled ground-water and surface-water FLOW model based on the integration of the precipitation-runoff modeling system (PRMS) and the modular ground-water flow model (MODFLOW-2005). U.S. Geological Survey Techniques and Methods 6-D1, 240 p

McIntyre NE, Wright CK, Swain S, Hayhoe K, Liu G, Schwartz FW, Henebry GM (2014) Climate forcing of wetland landscape connectivity in the Great Plains. Frontiers in Ecology and the Environment 12:59–64

Minor ES, Urban DL (2007) Graph theory as a proxy for spatially explicit population models in conservation planning. Ecological Applications 17:1771–1782

Mushet DM, Euliss NH, Stockwell CA (2012) Mapping anuran habitat suitability to estimate effects of grassland and wetland conservation programs. Copeia 2:321–330

Partington D, Brunner P, Frei S, Simmons CT, Werner AD, Therrien R, Maier HR, Dandy GC, Fleckenstein JH (2013) Interpreting streamflow generation mechanisms from integrated surface-subsurface flow models of a riparian wetland and catchment. Water Resources Research 49:5501–5519. doi:10.1002/wrcr.2040

Poiani KA, Johnson WC, Swanson GA, Winter TC (1996) Climate change and northern prairie wetlands: simulations of long-term dynamics. Limnology and Oceanography 41:871–881

Shaw DA, Van der Kamp G, Conly FM, Pietroniro A, Martz L (2012) The fill–spill hydrology of prairie wetland complexes during drought and deluge. Hydrological Processes 26:3147–3156

Sloan CE (1972) Ground-water hydrology of prairie potholes in North Dakota. U.S. Geological Survey Professional Paper 585-C

Therrien R, McLaren R, Sudicky E, Panday S (2010) HydroGeoSphere: a three-dimensional numerical model describing fully-integrated subsurface and surface flow and solute transport (manual). University of Waterloo, Waterloo

Winter TC (1978) Numerical simulation of steady state three-dimensional groundwater flow near lakes. Water Resources Research 14:245–254

Winter TC (ed) (2003) Hydrological, chemical, and biological characteristics of a prairie pothole wetland complex under highly variable climate conditions—the Cottonwood Lake Area, East-Central North Dakota. U.S. Geological Survey Professional Paper 1675

Woodhouse CA, Overpeck JT (1998) 2000 years of drought variability in the Central United States. Bulletin of the American Meteorological Society 79:2693–2714

Wright CK (2010) Spatiotemporal dynamics of prairie wetland networks: power-law scaling and implications for conservation planning. Ecology 91:1924–1930

Wright CK, Liu G, Schwartz FW, McIntyre NE, Swain S, Hayhoe K (2016) Simulated dynamics of prairie pothole habitat networks under low and high global warming scenarios. Wetlands (in this issue)

Yu Z, Schwartz FW (1998) Application of an integrated basin-scale hydrologic model to simulate surface-water and groundwater interactions. Journal of the American Water Resources Association 34:409–425

Yu Z, Pollard D, Cheng L (2006) On continental-scale hydrologic simulations with a coupled hydrologic model. Journal of Hydrology 331:110–124

Zhang B, Schwartz FW, Liu G (2009) Systematics in the size structure of prairie pothole lakes through drought and deluge. Water Resources Research 45:W04421. doi:10.1029/2008WR006878